A Novel Approach for Removing Decaying DC Offset from Fault Current Signals Using Cumulative Sum – Fast Moving Average (CumSum-FMA) Hybrid Algorithm

1st Philip Abel
Karlsruhe Institute of Technology (KIT)
Karlsruhe, Germany
philip.abel@kit.edu

2nd Friedrich Wiegel
Karlsruhe Institute of Technology (KIT)
Karlsruhe, Germany
friedrich.wiegel@kit.edu

3rd Michael Kyesswa
TenneT TSO
Bayreuth, Germany
michael.kyesswa@gmail.com

4th Simon Waczowicz
Karlsruhe Institute of Technology (KIT)
Karlsruhe, Germany
simon.waczowicz@kit.edu

5th Veit Hagenmeyer
Karlsruhe Institute of Technology (KIT)
Karlsruhe, Germany
veit.hagenmeyer@kit.edu

***Abstract*—This paper introduces an innovative hybrid methodology for removing decaying Direct Current Offset from fault current signals, a prevalent challenge in phasor estimation techniques in protective relay applications. Traditional techniques of solving this problem often fall short in efficiency and accuracy, especially when the faulty signal has complex non-linear decay patterns. Our method combines the Cumulative Sum and Fast-Moving Average techniques, utilizing the former's ability to track decaying Direct Current Offset trends and the latter's proficiency in smoothing signal variations. This approach not only enhances the accuracy of decaying Direct Current Offset removal but also preserves the integrity of the underlying signal. We demonstrate the superior performance of our method, highlighting its potential to significantly improve fault signal analysis and the reliability of power system operations.**

***Index Terms*—Direct Current Offset, Fault Current Signals, Protective Relays, Cumulative Sum Technique, Fast-Moving Average, Non-linear Decay Patterns, Power System Reliability.**

I. Introduction

In the dynamic landscape of power system engineering, the analysis of fault current signals stands as a cornerstone for maintaining the reliability and safety of power systems. However, a pervasive challenge in this domain is the presence of decaying Direct Current Offsets (DCOs) in fault signals.

This DCOs can significantly distort signal characteristics, leading to potential misinterpretations that jeopardize the effectiveness of transient stability assessments and the coordination of protective device.

A. Related Works

To get a full grasp of the state-of-the-art on DCO removal techniques, several published works on the subject matter were carefully perused. In [2], the authors presented a DCO removal algorithm using mimic filters. This approach is susceptible to error due to the impracticability of selecting desirable parameters of the mimic circuitry to match the time constant of the faulty signal. To overcome the drawbacks of traditional mimic filters, [6] reported an adaptive mimic filter algorithm whose reliability depends on the proper selection of cycle-count.

In [8], the authors presented an estimation scheme that combines Discrete Fourier Transform (DFT) with a Finte Impulse (FIR) notch filter. In the scheme, the output of the FIR notch filter, along with its complex conjugate, are used to obtain DCO parameters which are eventually subtracted from the initial DFT output. Although robust, the algorithm has a low rate of convergence and is less precise than conventional schemes. Insights on the use of Simpson's rule in estimating DCO were presented by [9]. In the study, the authors argue that parabolic approximation using Simpson's rule fits the curvatures of fault current signals with greater accuracy thereby making it a good fit for DCO estimation in fault current signals.

In [11], a DCO mitigation strategy using the moving average filter and the faulty signal's symmetry was presented. However, the test signal used in the study was devoid of frequency deviation and undesirable harmonic contents. Moreover, the algorithm's robustness is limited. In [17], a real-time DCO removal method using Morphological Median Filter (MMF) was presented. The study in [22] presented a method using full cycle Discrete Fourier Transform (FCDFT) and a second-order FIR notch filter for merging multiple DCOs into a single DCO, optimizing computation time with a quarter-sampling frequency.

Finally in [23], an Intrinsic Time-scale Decomposition tool was used to decompose a fault signal into Proper Rotation Components (PRC) and a monotonic trend signal that represent the DCO.

Due to the aformentioned problems, most of the DCO suppression/mitigation schemes yielded results that are less accurate and precise. Morever, the algorithms are less resilient and have low rate of convergence.

B. Contributions

To address the shortcomings enumerated in the previous section, we propose a novel hybrid method that amalgamates the Cumulative Sum and Fast-Moving Average techniques. This method is specifically tailored to tackle the nuanced challenges posed by DCO in fault current signals.

II. Mathematical Formulation of CumSum-FMA Algorithm

The Cumulative Sum component is adept at tracking the evolving trend of the DCO, proving especially beneficial in scenarios where the DCO has inherent non-linear characteristics. In parallel, the Fast-Moving Average technique is employed to effectively smooth out rapid signal variations, thereby facilitating a more accurate isolation of DCO components.

As per [2], [6], [8], fault current signal can be modelled using (1).

$$\begin{aligned} I[n] = \quad & A_0 e^{-\frac{n\Delta t}{\tau}} + A_1 \sin\left(n\delta + \theta_1\right) \\ & + \sum_{k=2}^{\frac{N}{2}-1} A_k \sin\left(kn\delta + \theta_k\right) \end{aligned} \tag{1}$$

In (1), n, N,τ, δ and Δt represent the number of samples, number of samples per cycle, DCO time constant, angular velocity and sampling interval respectively. Also, A_k and θ_k represent the amplitudes and phase angle of the k^{th} harmonic component. The corrected fault signal can be obtained using (2).

$$I_{\text{corrected}}\left[n\right] = I_{\text{discrete}}\left[n - \frac{N}{2}\right] - I_{\text{ma}}\left[n\right] \tag{2}$$

where

$$I_{\text{ma}}[n] = \frac{\text{Cumsum}[n] - \text{Cumsum}[n-N]}{N}, \forall n \geq N \tag{3}$$

$$\text{Cumsum}[n] = \sum_{k=1}^{n} x[k] \tag{4}$$

$$\text{Cumsum}[n-N] = \sum_{k=1}^{n-N} x[k] \tag{5}$$

By combining Eq. (4) and Eq. (5), we can obtain Eq. (6)

$$I_{ma}[n] = \frac{1}{N}\left(\sum_{k=n-N+1}^{n} x[k]\right), \forall n \geq N \tag{6}$$

A. Analytic Illustration of DCO Removal using the proposed algorithm

As per (2), the discretized part of the fault signal can be expressed as follows:

$$\begin{aligned} I_{\text{discrete}}\left[n - \frac{N}{2}\right] = \ & A_0 e^{-\frac{\left(n-\frac{N}{2}\right)\Delta t}{\tau}} \\ & + A_1 \sin\left(\left(n - \frac{N}{2}\right)\delta + \theta_1\right) \\ & + \sum_{k=2}^{\frac{N}{2}-1} A_k \sin\left(k\left(n - \frac{N}{2}\right)\delta + \theta_k\right) \end{aligned} \tag{7}$$

Furthermore, the right hand side of (2), can be evaluated as follows:

$$I_{\text{ma}}\left[n\right] = I_{\text{maexp}}\left[n\right] + I_{\text{masin}}\left[n\right] \tag{8}$$

The moving average of each sinusoidal component tends to zero over periods where N is an integer multiple of the sinusoid's period. As such,

$$I_{\text{masin}}\left[n\right] \approx 0 \tag{9}$$

Now, the moving average of the exponential term can be expressed as in (10).

$$I_{\text{maexp}}\left[n\right] = \frac{1}{N}\sum_{i=n-N+1}^{n} A_0 e^{-\frac{i\Delta t}{\tau}} \tag{10}$$

In the interval from $n-N+1$ to n, the midpoint is at $n - \frac{N}{2}$. For small intervals, the sum of exponentials can be approximated by multiplying the number of terms N by the exponential at the midpoint [1], [4] and [5]. Thus,

$$\sum_{i=n-N+1}^{n} e^{-\frac{i\Delta t}{\tau}} \approx N \cdot e^{-\frac{\left(n-\frac{N}{2}\right)\Delta t}{\tau}} \tag{11}$$

Plugging (11) in (10) yields

$$I_{\text{maexp}}[n] \approx \frac{1}{N} \cdot N \cdot A_0 e^{-\frac{\left(n-\frac{N}{2}\right)\Delta t}{\tau}} \tag{12}$$

Thus,

$$I_{ma}[n] \approx A_0 e^{-\frac{\left(n-\frac{N}{2}\right)\Delta t}{\tau}} \tag{13}$$

Putting (7) and (13) in (2) yields

$$\begin{aligned} I_{\text{corrected}}\left[n\right] = \quad & A_1 \sin\left(\left(n - \frac{N}{2}\right)\delta + \theta_1\right) \\ & + \sum_{k=2}^{\frac{N}{2}-1} A_k \sin\left(k\left(n - \frac{N}{2}\right)\delta + \theta_k\right) \end{aligned} \tag{14}$$

The time constant of the decaying exponential DC and its amplitude can be estimated using (15) and (16) as per [3]. It is important to note that $\text{S}[n] = \sum_{n=N_1}^{N_2} I[n]$.

$$\tau = -\frac{\Delta n \Delta t}{\ln\left(\frac{S[n+\Delta n]}{S[n]}\right)} \tag{15}$$

$$A_0 = \frac{S[n]}{\sum_{n=N_1}^{N_2} e^{-\frac{n\Delta t}{\tau}}} \tag{16}$$

III. Illustrative Implementation of the Proposed Algorithm as Hybrids

The proposed algorithm was hybridized with the Kalman Filter (pKF) to illustrate the hybrid implementation. As per [7], the corrected signal can be expressed as in (17). For the first two harmonics, (20)-(27) represents the proposed algorithm - Kalman Filter hybrid implementation. The magnitude and the phase angles of respective harmonic components can be obtained using (29) and (30).

$$I_{\text{corrected}}\left((k+1)\Delta t\right) = H \cdot F \cdot X(k) \tag{17}$$

where

$$H = \begin{bmatrix} 1 & 0 & 1 & 0 \end{bmatrix} \tag{18}$$

$$F = \begin{bmatrix} \cos(\omega_0\Delta t) & -\sin(\omega_0\Delta t) & 0 & 0 \\ \sin(\omega_0\Delta t) & \cos(\omega_0\Delta t) & 0 & 0 \\ 0 & 0 & \cos(2\omega_0\Delta t) & -\sin(2\omega_0\Delta t) \\ 0 & 0 & \sin(2\omega_0\Delta t) & \cos(2\omega_0\Delta t) \end{bmatrix} \tag{19}$$

$$X_{k|k-1} = FX_{k-1|k-1} \tag{20}$$

$$P_{k|k-1} = FP_{k-1|k-1}F^T + Q \tag{21}$$

$$Y_{\text{pred}} = HX_{k|k-1} \tag{22}$$

$$e = I_{\text{corrected}} - Y_{\text{pred}} \tag{23}$$

$$S = HP_{k|k-1}H^T + R \tag{24}$$

$$K = P_{k|k-1}H^T S^{-1} \tag{25}$$

$$X_{k|k} = X_{k|k-1} + Ke \tag{26}$$

$$P_{k|k} = (I - KH)P_{k|k-1} \tag{27}$$

$$X[k] = \begin{bmatrix} A_1\cos(\theta_1) \\ A_1\sin(\theta_1) \\ A_2\cos(\theta_2) \\ A_2\sin(\theta_2) \end{bmatrix} \tag{28}$$

$$A[k] = \sqrt{X_{2k}[k]^2 + X_{2k+1}[k]^2} \tag{29}$$

$$\theta(k) = \tan^{-1}\left(\frac{X_{2k+1}[k]}{X_{2k}[k]}\right) \tag{30}$$

In the above formulations, $X_{2k}[k]$ and $X_{2k+1}[k]$ are the estimated cosine and sine coefficients of each harmonic component at time step k. F, Q, P, I, H, e, R, and S represent the state transition, process noise covariance, covariance, identity, measurement, measurement residual, measurement noise covariance, and innovation covariance matrices respectively. Also, Y_{pred} and K denotes the predicted measurement vector, and Kalman gain respectively. Finally, $X_{k|k-1}$ and $X_{k|k}$ represent the predicted and updated state estimates

IV. Simulation Setup

The effectiveness of our method was tested on a test-network represented in Fig. 1. In the figure, a, b (i.e. b1 and b2), c, d, e, f, g, h, i, j and k represent part of a distribution network, designated nodes, circuit breaker (CB), line, current transformer (CT), fault, relay, DGs (Solar Power Plant, Wind Power Plant and Solar Power Plant) and nonlinear load respectively. The fault current in the primary and secondary sides of the CT are denoted by $I_{f_{prim}}$ and $I_{f_{sec}}$. The simulated signals were generated to mimic typical fault scenarios with varying degrees of DCO. The parameters of the test network are presented in Table I.

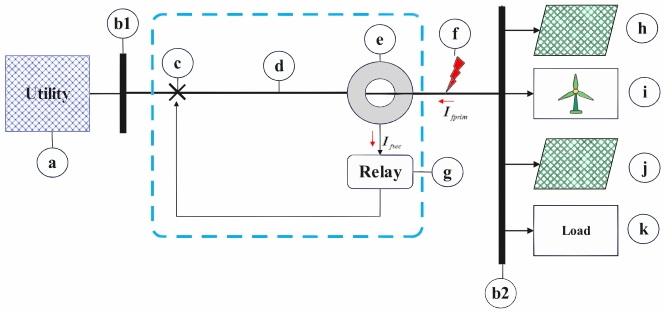

Fig. 1: Single Line Diagram of the test system

TABLE I: Parameter of the test system

EPS	$S_c = 250MVA, U = \frac{25}{\sqrt{3}}$[kV]
Line	$l = 5.8$ km, $[r_1, r_0] = [0.012730, 0.3864]$[Ω/km]
	$[l_1, l_0] = [0.9337e-3, 4.1264e-9]$[H/km]
	$[c_1, c_0] = [12.74e-9, 7.751e-9]$[C/km]
Fault	$l_f = 60\% \times l, t_{sw} = [0.20, 0.4]$[s], $R_s = 1e6$[Ω]
	$R_g = 0.001$[Ω], $R_{on} = 0.001$[Ω]
Plants / Loads	$2 \times 1.5MW$ Photovoltaic Plant
	$4.5MW$ Windfarm
	$2MW$ Nonlinear load

In Table I, $[r_1, r_0], [l_1, l_0]$ and $[c_1, c_0]$ represents the positive- and zero-sequence resistances, inductance and capacitance of the line per unit distance respectively. Also, S_c, U, t_{sw} and l, l_f, R_{on}, R_g, R_s denotes the short circuit level of the grid part, the grid voltage, the switching time, length of line, distance of fault on line, fault resistance, ground resistance, and snubber resistance respectively.

Fig. 2. shows the operation of candidate estimators using the time-window method [1]. The terms $w1$ to $w4$ stand for respective time-window number [1]. The time-window number can be extended to wk window in line with design trade-offs. The discriminatory capabilities of the relay hinges on effective estimation of the magnitude of the fundamental frequency component.

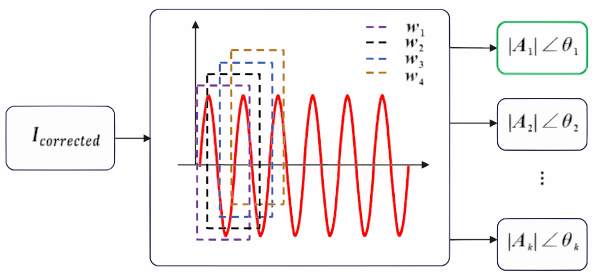

Fig. 2: Estimation process by Estimators

V. Simulation Results

The proposed algorithm was implemented in conjuction with other algorithms as hybrids in the test-network. The results obtained for the Kalman Filter (KF) [7], Least Square Error (LSE) [1], Full cycle Discrete Fourier Transform (FCDFT) [1], [8], and the Modified Cosine Filter (MCF) [11] (Fig. 3 - Fig. 6) shows the superiority of hybrid schemes based on the proposed algorithm in terms of the stability in the values of the fundamental frequency components estimated.

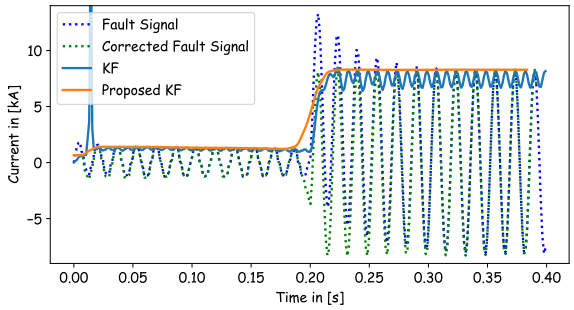

Fig. 3: Kalman Filter vs proposed-Kalman Filter

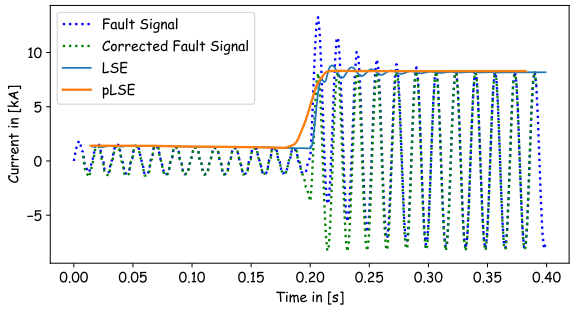

Fig. 4: LSE vs proposed-LSE (pLSE)

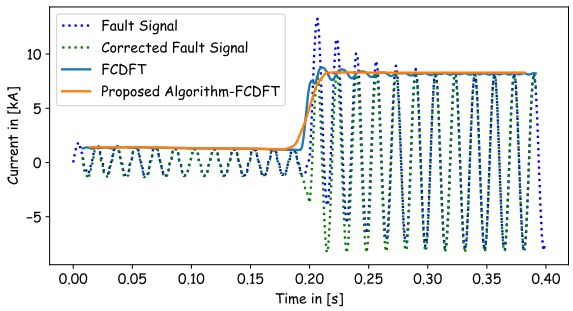

Fig. 5: FCDFT vs proposed-FCDFT (pFCDFT)

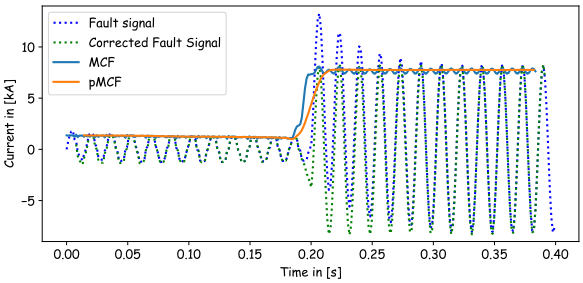

Fig. 6: MCF vs proposed-MCF (pMCF)

VI. Performance Evaluation Metrics (PEM)

The performance of the proposed algorithm was investigaed using four metrics [2] as in (31) - (34).

$$\text{MAE} = \frac{1}{N}\sum_{i=1}^{N}|y_i - \hat{y}_i| \tag{31}$$

$$\text{Precision } = \frac{1}{\text{Var}(\hat{y})} \tag{32}$$

$$|\,\text{RoC}\,| = \min\{k : |y_k - \hat{y}_k| < \varepsilon\} \tag{33}$$

$$\text{Robustness } (y, \hat{y}, \tilde{y}) = \frac{MAE\,(y_\text{i}, \hat{y}_\text{i})}{MAE\,(y_\text{i}, \tilde{y}_\text{i})} \tag{34}$$

The terms MAE, RoC, y_i, $\hat{y}_i$, $\tilde{y}_\text{i}$, N, ε and $Var(\hat{y})$ represents Mean Absolute Error (i.e. measure of accuracy), Rate of Convergence, true values, estimated values, noisy predicted values, number of samples, predefined error threshold, and the variance of the estimated values respectively.

The robustness analysis provided insights into each method's ability to maintain accuracy despite the introduction of noise, revealing a range of resilience among the methods. Precision also varied across the methods, underscoring the consistency and reliability of certain techniques over others.

The PEM results for the FCDFT, Adaptive Mimic Filter-Full Cylcle Discrete Fourier Transform (adMimic-FCDFT) [6], Kalman Filter (KF) [7], Modified Cosine Filter (MCF), Least Square Error (LSE) [1] and Recursive Least Mean Square (RLMS) [1] are presented in Fig. 7 - 9.

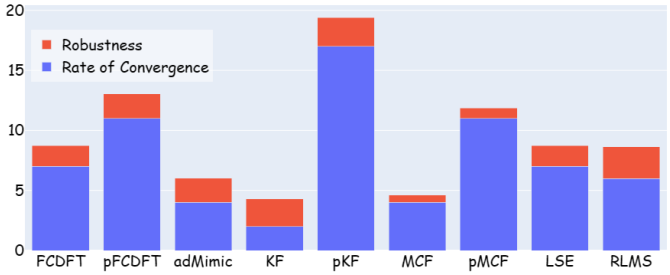

Fig. 7: Robustness and RoC of different schemes

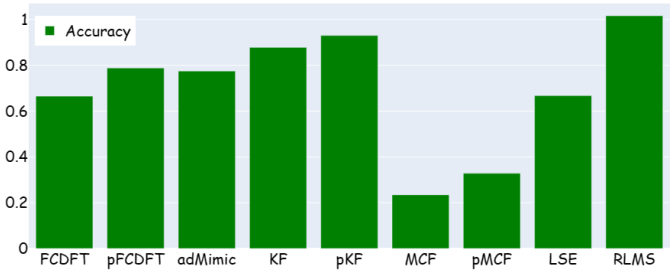

Fig. 8: Accuracy of different schemes

Fig. 9: Precision of different schemes

VII. Discussions/Data Analysis

The PEM result revealed notable improvements in rate of convergence, robustness (Fig. 7) and precsion (Fig. 9) in hybrid schemes based on the proposed algorithm indicating improvement in better efficiency over others schemes. Furthermore, there was recorded improvement in the accuracy (Fig. 8) of the hybrid schemes using the proposed method. The rate of convergence had significant impacts on the computational burden and time.

VIII. Conclusion

Overall, algorithm-hybrids based on the suggested method demonstrated better performance than most of the methods investigated. The PEM findings of this study can be instrumental in aiding future design trade-offs. Future work will focus on refining the technique and exploring its applications in other domains.

Acknowledgment

This project is funded by the Helmholtz Association under the Program “Energy System Design”.

References

[1] Hayes, Monson H.. “Statistical Digital Signal Processing and Modeling.” (1996).

[2] G. Benmouyal, “Removal of DC-offset in current waveforms using digital mimic filtering,” in IEEE Transactions on Power Delivery, vol. 10, no. 2, pp. 621-630, April 1995, doi: 10.1109/61.400869.

[3] Cho, Yoon-Sung, et al., “An innovative decaying DC component estimation algorithm for digital relaying,” Power Delivery, IEEE Transactions on 24.1, 2009: 73-78.

[4] Sukparungsee S, Areepong Y, Taboran R (2020) “Exponentially weighted moving average—Moving average charts for monitoring the process mean”. PLOS ONE 15(2): e0228208. https://doi.org/10.1371/journal.pone.0228208

[5] Mao, Lei. “Exponential Moving Average.” https://leimao.github.io/blog/Exponential-Moving-Average/.

[6] N. L. S. Oliveira and B. A. de Souza, “Effects of the exponentially decaying DC offset in the phasor estimation algorithms performance,” 2012 Sixth IEEE/PES Transmission and Distribution: Latin America Conference and Exposition (T&D-LA), Montevideo, Uruguay, 2012, pp. 1-5, doi: 10.1109/TDC-LA.2012.6319090.

[7] Bukh, Bjarne et al. “Advantages in using Kalman phasor estimation in numerical differential protective relaying compared to the Fourier estimation method.” (2007).

[8] Afrandideh, Saeed.“A Modified DFT-Based Phasor Estimation Algorithm Using an FIR Notch Filter.” IEEE Transactions on Power Delivery 38 (2023): 1308-1315.

[9] Kumar, Bandi Ravi et al. “Key Insights on Methods for Estimation of Decaying DC Component in Fault Currents.” 2022 22nd National Power Systems Conference (NPSC) (2022): 848-853.

[10] Mohammadi, Sina et al. “Decaying DC Offset Current Mitigation in Phasor Estimation Applications: A Review.” Energies (2022).

[11] Menezes, Thiago S. et al. “Moving average-based mitigation of exponentially decaying DC components.” Electric Power Systems Research (2023).

[12] Mohammadi, Sina et al. “A novel analytical method for DC offset mitigation enhancing DFT phasor estimation.” Electric Power Systems Research (2022).

[13] Allahbakhshi, Mehdi et al. “Hybrid approach for immunisation of DFT-based phasor estimation method against decaying DC components.” IET Science, Measurement & Technology (2019).

[14] Rozgic, Dimitrije and Predrag Bosko Petrovic. “New Procedure for Estimation of Power Fundamental Phasor Parameters in Presence of Decaying DC Components.” WSEAS TRANSACTIONS ON POWER SYSTEMS (2022).

[15] Kim, Woo-Joong et al. “Adaptive Phasor Estimation Algorithm Based on a Least Squares Method.” Energies (2019).

[16] Yu, Haotian et al. “A Phasor Estimation Algorithm Robust to Decaying DC Component.” IEEE Transactions on Power Delivery 37 (2021): 860-870.

[17] Godse, Revati and Sunil Bhat. “Real-time digital filtering algorithm for elimination of the decaying DC component using mathematical morphology.” IET Generation, Transmission & Distribution (2019).

[18] Sardari, Hadi et al. “Fast DC Offset Removal for Accurate Phasor Estimation using Half Cycle Data Window.” (2022).

[19] Kumar, Bandi Ravi et al. “A Novel Sub-Cycle-Based Method for Estimation of Decaying DC Component and Fundamental Phasor.” IEEE Transactions on Instrumentation and Measurement 70 (2021): 1-10.

[20] Lu, Dian et al. “Generalized Phasor Estimation Method Based on DFT with DC Offset Mitigation.” 2021 IEEE Power & Energy Society General Meeting (PESGM) (2021): 1-5.

[21] Tajdinian, Mohsen et al. “An analytical approach for removal of decaying DC component considering frequency deviation.” Electric Power Systems Research 130 (2016): 208-219.

[22] Hwang, Jin Kwon et al. “DFT-Based Phasor Estimation for Removal of the Effect of Multiple DC Components.” IEEE Transactions on Power Delivery 33 (2018): 2901-2909.

[23] Pazoki, Mohammad. “A New DC-Offset Removal Method for Distance-Relaying Application Using Intrinsic Time-Scale Decomposition.” IEEE Transactions on Power Delivery 33 (2018): 971-980.